Metabolic Brain Disease (2019) 34:1117–1130
https://doi.org/10.1007/s11011-019-00433-0

ORIGINAL ARTICLE

Schwann cell transplantation exerts neuroprotective roles in rat model of spinal cord injury by combating inflammasome activation and improving motor recovery and remyelination

Mahboubeh Mousavi[1] · Azim Hedayatpour[1] · Keywan Mortezaee[2] · Yousef Mohamadi[3] · Farid Abolhassani[1] · Gholamreza Hassanzadeh[1]

Received: 21 August 2018 / Accepted: 13 May 2019 / Published online: 4 June 2019

Abstract

Inflammasome activation in the traumatic central nervous system (CNS) injuries is responsible for propagation of an inflammatory circuit and neuronal cell death resulting in sensory/motor deficiencies. NLRP1 and NLRP3 are known as activators of inflammasome complex in the spinal cord injury (SCI). In this study, cell therapy using Schwann cells (SCs) was applied for targeting NLRP inflammasome complexes outcomes in the motor recovery. These cells were chosen due to their regenerative roles for CNS injuries. SCs were isolated from sciatic nerves and transplanted to the contusive SCI-induced Wistar rats. NLRP1 and NLRP3 inflammasome complexes and their related pro-inflammatory cytokines were assayed in both mRNA and protein levels. Neuronal cell survival (Nissl staining), motor recovery and myelination (Luxol fast blue/LFB) were also evaluated. The groups were laminectomy, SCI, vehicle and treatment. The treatment group received Schwann cells, and the vehicle group received solvent for the cells. SCI caused increased expressions for both NLRP1 and NLRP3 inflammasome complexes along with their related pro-inflammatory cytokines, all of which were abrogated after administration of SCs (except for IL-18 protein showing no change to the cell therapy). Motor deficits in the hind limb, neuronal cell death and demyelination were also found in the SCI group, which were counteracted in the treatment group. From our findings we conclude promising role for cell therapy with SCs for targeting axonal demyelination and degeneration possibly through attenuation of the activity for inflammasome complexes and related inflammatory circuit.

Keywords Spinal cord injury (SCI) · NLRP · Inflammation · Schwann cells

✉ Farid Abolhassani
abolhasf@sina.tums.ac.ir

✉ Gholamreza Hassanzadeh
hassanzadeh@tums.ac.ir

Mahboubeh Mousavi
Msmousavi85@gmail.com

Azim Hedayatpour
hedayatpour@sina.tums.ac.ir

Keywan Mortezaee
mortezaee.k@muk.ac.ir; keywan987@yahoo.com

Yousef Mohamadi
Yosef.1365@yahoo.com

[1] Department of Anatomy, School of Medicine, Tehran University of Medical Sciences, Tehran, Iran

[2] Department of Anatomy, School of Medicine, Kurdistan University of Medical Sciences, Sanandaj, Iran

[3] Department of Anatomy, School of Medicine, Ilam University of Medical Sciences, Ilam, Iran

Introduction

Spinal cord injury (SCI) is a dangerous lesion that occurs due to traumatic or non-traumatic damages and result in sensory and motor deficits (Choobineh et al. 2016; Mortezaee et al. 2018) The incidence of SCI was reported more than 2.36/10000 cases with mean age of 29.1 years in Iran, according to Specialized Spinal cord injury center in Tehran (Choobineh et al. 2018; Mortazavi et al. 2015). SCI can lead to serious complications and death in some cases due to its pathophysiology and the lack of adequate therapies (Gholaminejhad et al. 2017; Martinon et al. 2002).

Therefore, studying the mechanisms involved in SCI is essential to develop appropriate therapeutics. The pathological changes that are developed following SCI are divided into two steps of primary and secondary insults (Nikmehr et al. 2017). In primary injury, which occurs within a few minutes of injury, impaired neural and endothelial tissues due to hemorrhagic necrosis are observed mainly in the spinal cord gray matter.

These alterations leads to wide range of neural complications such as paraplegia and quadriplegia (Sekhon and Fehlings 2001). Secondary damages, which happens in many cases, are recognized following electrolyte imbalances, microvascular damages and edema, free radical production, excitotoxicity, demyelination, neuroinflammation and late cell death (Anderson et al. 1982; Pishva et al. 2016). These conditions lead to a series of problems such as urinary tract dysfunctions, cardiovascular and respiratory diseases and also cause up to a maximum of 16.7% of morbidity and mortality (Norenberg et al. 2004; Profyris et al. 2004; Zhang et al. 2013).

Neuroinflammation is well known response involved in the pathogenesis of several CNS disorders (Hassanzadeh et al. 2016; Pishva et al. 2016). Inflammasome was first identified by Tschopp et al. in THP1 cells in 2002 (Martinon et al. 2002). Inflammasomes are multiprotein complexes which act as a key element of the innate immune system. (Tschopp and Schroder 2010). These complexes are sensors for pathogen-associated molecular patterns (PAMPs) or damage-associated molecular patterns (DAMPs) that, in turn, are recognized by pattern recognition receptors (PRRs). There are four known clades for PRRs: C-type lectins (CTLs), membrane-bound, retinoic acid–inducible gene (RIG)-I-like receptors (RLRs), Toll-like receptors (TLRs) and the nucleotide-binding domain leucine-rich repeats (NLRs). NLRs are intracellular proteins and components for certain types of inflammasomes like NLRP1 and NLRP3 (Mortezaee et al. 2018). Each inflammasome has three main components: a cytoplasmic sensor, an adaptor protein and an effector caspase (Fleshner et al. 2017). NLRs are cytoplasmic sensors, and apoptosis-associated speck-like protein (ASC) and caspase-1 are adaptor and effector proteins, respectively (Fleshner et al. 2017; Zendedel et al. 2016). Upon inflammasome activation, the NLR component is attached to caspase-1 by ASC that is followed by cleavage of caspase-1 and activation of pro-inflammatory cytokines including tumor necrosis factor-α (TNF-α), interleukin-1β (IL-1β), and IL-18 (Bazrafkan et al. 2018; Bergsbaken et al. 2009). Caspase-1 is also a mediator for a unique form of neuronal cell death called pyroptosis (Mortezaee et al. 2018).

Many therapeutic procedures have been exploited so far for attenuating lesion-mediated disturbances with a special focus on neuroinflammation and related cascades. Among them, cell therapy using stem- or non-stem cells is an approach for this contex (Mortazavi et al. 2015). Schwann cells (SCs) are myelin producers in the peripheral nervous system (PNS), and that they are also known for their beneficial roles in regeneration of injured axons in the CNS (Deng et al. 2015). Myelin forming SCs contribute in CNS regeneration through release of growth factors, expression of cell adhesion molecules (CAMs), production of extracellular matrix (ECM) molecules (Mirsky et al. 2002), activation and migration of macrophages for phagocytosis of myelin debris (Arthur-Farraj et al. 2012), and postponing glial scar formation (Kuo et al. 2011). Additionally, the use of SCs in clinical trials reveals the safety and potency of these cells in engraftments alone (Saberi et al. 2011; Zhou et al. 2012) or in conjunction with other cells (Chen et al. 2014; Oraee-Yazdani et al. 2016).

There are many debates about interaction of SCs and their neuroinflammatory role in diseases. Some studies indicate that under neuroinflammation, activated SCs express PRRs that give them the ability to detect pathogens, to proliferate, to phagocyte myelin debris and to support regeneration of axons (Campana 2007; Tofaris et al. 2002). These cells also produce anti-inflammatory cytokines to prevent overactivation of the immune responses (Taskinen et al. 2000; Zhang et al. 2011). Beside these essential roles for SCs on amelioration of the neuroinflammatory diseases, they also produce pro-inflammatory cytokines such as IL-1β, TNF-α, IL-6 (interleukin-6), chemokines such as leukemia inhibitory factor (LIF) and monocyte chemoattractant protein (MCP)-1 as well as nitric oxide, adhesion molecules and many more (Shamash et al. 2002; Shen et al. 2008; Tofaris et al. 2002). Under the induction of chemoattractants, immune cells infiltrate into the injured sites and amplify the immune responses (Dubový 2011) leading to the aggravation of neuroinflammation. Existence of these dual roles for SCs in neuroinflammatory diseases led us to design the present study in order to gain an understanding of a possible effect of intrathecal injections of SCs on activation of the NLRP multiprotein complexes, and on motor recovery and remyelination in the rat model of SCI.

Methods and materials

Animals and surgical procedure

32 male adult Wistar rats (250–300 g) were purchased from Pasteur Institute of Iran. The animals were housed in an environmentally-controlled conditions (illumination, 12/12 light/dark cycle; humidity, 50–60%; and temperature: 21–23 °C), and had easy access to food and water. All procedures were carried out in keeping with the Guidelines from Tehran University of Medical Sciences for animal use and care. Animals were randomly divided into four groups ($n = 8$): sham (laminectomy), SCI, vehicle, and treatment. Sham-operated group only had laminectomy, vehicle group received basal medium, and treatment group received Schwann cells.

SCI model was made using a weight compression method as previously published (Zendedel et al. 2016). First, animals were anesthetized by intraperitoneal (IP) injection of a cocktail of ketamine (80 mg/kg) and xylazine (10 mg/kg). Required anesthetic level was tested with the absence of pedal response to a hard pinch. After shaving the surgical area, they were placed on a board ventrally, and their limbs were

tightened with elastic bands in order to hold the spinal column in a flat direction. Skin incision was made over spinous processes T9-T11, blunt dissection of muscles was performed. Using fine rongeur, dorsal laminectomy of T10 vertebra was performed without disturbing the dura matter. Then, a metal rod with a rectangular shape weighing 50 g was placed in contact area with spine (2.2 × 5.0 mm [11.0 mm^2]) for making a compression on the cord. Immediate responses to compression are congestion in the injured area and withdrawal of the tail and hind limbs. This congestion along with tremor in the hind limbs, rapid contraction and incontinence are confirmative signs for exploiting a successful SCI model. When the contusive model met the demanded time (5 min), muscles and overlying skin were sutured. Sham-operated animals were only had laminectomy. During the surgery, room temperature was controlled, and all procedures were carried out under sterile conditions. After surgery, all animals received intramuscular injection of 6 mg/kg gentamycin (Caspiantamin, Iran) for three consecutive days and subcutaneous injection of 2 mL sterile saline 0.09% to prevent infection and rehydration respectively. Manual bladder drainage was another after care for these animals due to impaired bladder function caused by spinal shock. This drainage was performed twice daily until recovery of bladder function.

Schwann cell isolation and culture

SCs were obtained from sciatic nerve of 2–3 day-old Wistar rats according to Kreider et al. (Kreider et al. 1981) with minor modification. In brief, sciatic nerves between the hip and knee joints were cut bilaterally and kept in ice-cold phosphate-buffered saline (PBS; Dulbecco A, Oxoid) plus 100 U/ml penicillin (Gibco, USA) and 100 μg/ml streptomycin (Gibco, USA). Epineurium and other structures like muscles and vessels were removed. Nerves were cut into 1 mm pieces. The nerve pieces were then transferred into 15 mL tubes containing 0.25% trypsin-EDTA (Sigma, Germany) and 0.03% collagenase type-I (Sigma, Germany) in an incubator (37 °C and 5% CO_2), and mechanical dissociation of the pieces was performed using a glass Pasteur pipette for every 10 min. Samples, were then centrifuged (for 3 min at 2000 rpm, room temperature), and transferred into 25-cm^2 poly-L-lysine-coated culture flasks with fresh feeding medium containing 10 ml fetal calf serum (FCS) (Gibco, USA), Eagles MEM with Hank's salts (Gibco, USA), penicillin, streptomycin, 10 ng/ ml fibroblast growth factor (FGF)-2 (Sigma, Germany) + 1% (*v*/v) N2 supplement (Thermo Fisher Scientific, USA) and kept in cell culture incubator. The medium was replaced every two days. After receiving a suitable confluence (80%–85%), SCs were trypsinized with 0.25% Trypsin-EDTA, centrifuged (6 min, at 4000 rpm, room temperature) and passaged. SCs at passage three were used for further experiments.

Immunocytochemistry (ICC) of Schwann cells

SCs were identified using ICC method. For this purpose, the cells were fixed in 4% paraformaldehyde (pH 7.4) for 15 min. Then, they were washed with 0.1 M PBS and exposed to a blocking solution containing 0.1 M PBS, 0.3% Triton X-100 and 1% normal goat serum for 30 min. Incubation **w**ith primary mouse anti-S100 antibody (Abcam, Germany) was done overnight at 4 °C. After washing with PBS, SCs were incubated with AlexaFluor 488-conjugated secondary goat anti-mouse antibody (Abcam, Germany) at room temperature for 3 h in dark. Cell nuclei were counterstained with 10 μg/ml propidium iodide (PI, Sigma, Germany) dye in PBS for 30 min at 37 °C. Finally, SCs were observed under a fluorescent microscope (Olympus AX 70, Japan).

Flow cytometry analysis

The identity and purity of SCs were evaluated by assessing their surface markers. The cells were incubated with monoclonal antibodies including PE-conjugated rat anti-Thy-1 (CALTAG, USA), PE-Cy5-congjugated rat anti-CD45 (eBioscience, USA), and fluorescein isothiocyanate (FITC)-conjugated antibodies against P75 NLGFr and S100 (both from Invitrogen, USA) at 4 °C for 30 min. Thy-1 and CD45 antibodies were used for fibroblast depletion assay, P75 NLGFr and S100 antibodies were used as positive markers for Schwann cells. Finally, the cells were twice washed with FCS and analyzed by a FACS Calibur flow-cytometer (BDBiosciences, USA).

CM-Dil labeling of Schwann cells

SCs were labeled with a fluorescent lipophilic cell tracker called 1, 1′- dioctadecyl-3, 3, 3′, 3′ tetramethylindocarbocyanin perchlorate (C7000, Molecular Probes™, USA). SCs were detached from culture flask using 0.25% Trypsin-EDTA, washed in PBS and centrifuged at 1200 rpm for 10 min. Then, a number of 10^6 cells were exposed to 4 μM CM-Dil/mL medium. SCs were incubated for 5 min in a humidified incubator (5% CO2/95% O2) at 37 °C followed by an additional incubation for 15 min at 4 °C. The labeled cells were kept in ice before injection.

Schwann cell transplantation

At 1 week after SCI, Schwann cell transplantation was performed by adhering to the previous published procedure with slight modifications (De la Calle and Paíno 2002). Prior to cell transplantation, Trypan Blue vital dye diluted in 20 μL d H_2O was injected into the lumbar cistern of L3-L5 lumbar vertebra using a 20 μL Hamilton syringe (26 s G needle, Hamilton, USA), and delivery of this dye into subarachnoid space was

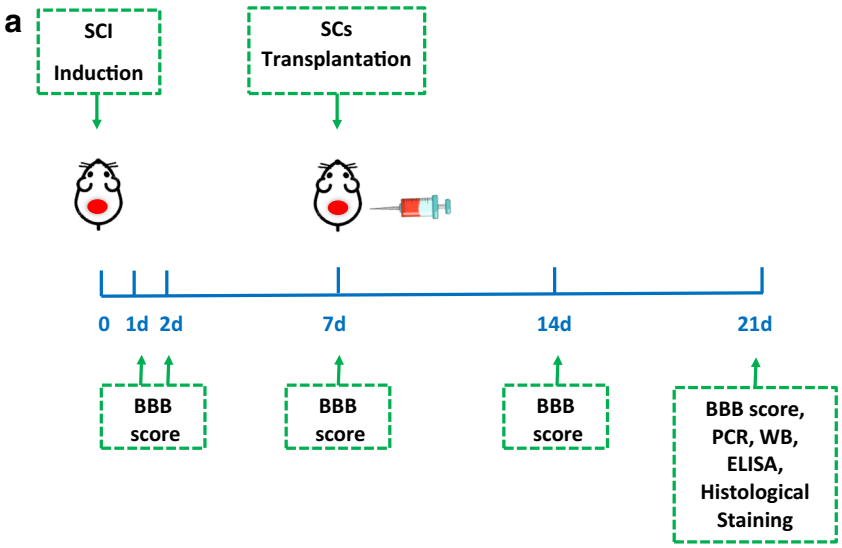
a
SCI Induction
SCs Transplantation
0 1d 2d
7d
14d
21d
BBB score
BBB score
BBB score
BBB score, PCR, WB, ELISA, Histological Staining

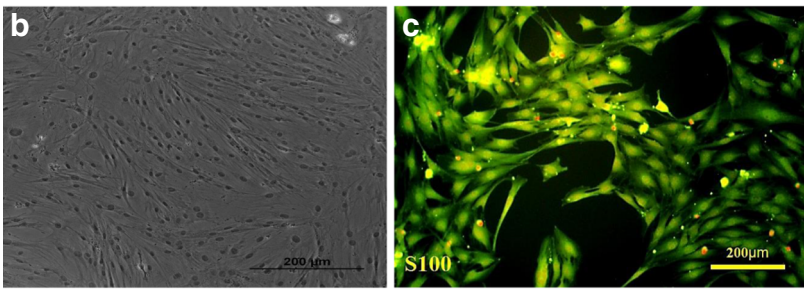
b
200 μm
c
S100
200μm

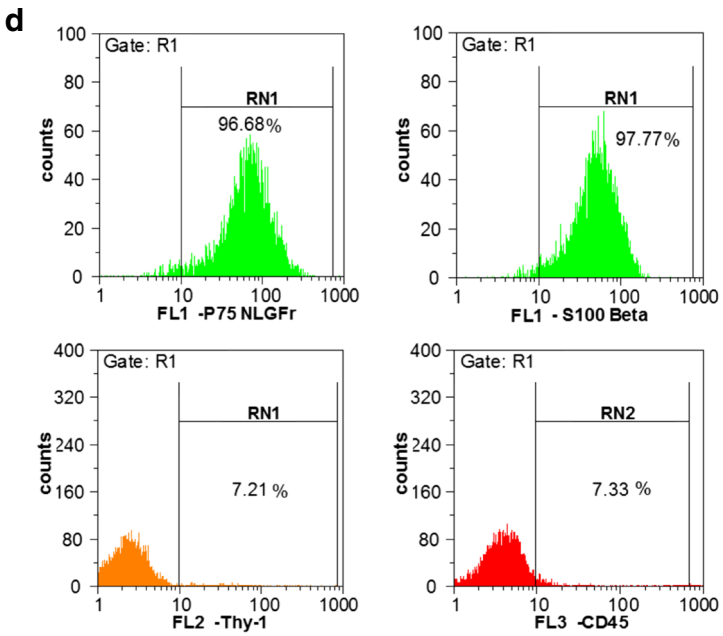
d
Gate: R1
RN1
96.68%
counts
FL1 -P75 NLGFr
Gate: R1
RN1
97.77%
FL1 - S100 Beta
Gate: R1
RN1
7.21 %
FL2 -Thy-1
Gate: R1
RN2
7.33 %
FL3 -CD45

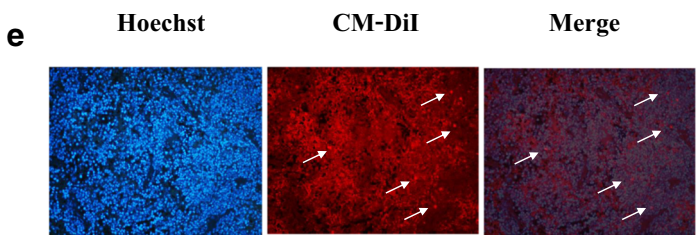
e
Hoechst
CM-DiI
Merge

◀ **Fig. 1** Time line of experiments and morphological characteristics of rat Schwann cells. **a** at the beginning of the study (on day 0), SCI model was made using a weight compression method. Then behavioral assessment (BBB) was assessed on days 1, 2, 7, 14 and 21 post-injury. At the end of experiment, after rating locomotor activity, all animals were sacrificed and real-time quantitative PCR, western blotting (WB), enzyme-linked immunosorbent assay (ELISA) and histological staining (Nissl and Luxol Fast Blue) were performed. **b** After 3 weeks of cultivation, cultured Schwann cells appeared small, bi- or tripolar elongated morphology. By contrast, fibroblasts displayed flat polymorphic appearance with larger nuclei. **c** Immunocytochemistry (ICC) for Schwann cells. The cells were S100 positive and nuclei stained with PI (yellow). **d** Flow cytometry analysis of Schwann cells for surface markers. The cells were positive for P75 NLGFr and S100, but negative for CD45 and CD90. **e** Cross section of rat spine at 1 week after transplantation of CM-Dil labeled Schwann cells. Labeled Schwann cells were seen as bright red points in subarachnoid space attached to the pia matter and injured zones of the spinal cord. Scale bars: 300 μm

then traced. This was performed in order to ascertain the correct place for cell delivery. SCs were collected from culture flasks using 0.25% Trypsin-EDTA and centrifuged (4000 rpm for 6 min).

In the next step, animals were placed on a surgical board, and their forelimbs were tightened with elastic bands, but their hind limbs were left to hang off. The area in the skin over L3-L5 area was shaved and scrubbed with povidone-iodine. On this area, a longitudinal incision (1.5 cm length) was made, and fascia and paravertebral muscles were excised and retracted. Then, administration of 3×10^5 CM-Dil-labeled SCs in 10 μL basal medium was performed using a 10 μL Hamilton syringe (26 s G needle, Hamilton, USA). Vehicle group only received 10 μL of basal medium. At 1 week after cell injection, homing of the cells into injured area was assayed fluorescently under a fluorescent microscope (Olympus, Japan). Timeline of study procedure is shown in the Fig. 1a.

Behavioral test

The Basso, Beat- tie and Bresnahan (BBB) locomotor rating scale was used for assessment of locomotor activity in the hind limbs according to the previously published work (Basso et al. 1996). For this purpose, open-field locomotion area was observed by two independent testers who were blinded to the experimental treatment for 5 min on days 1, 3 and 7 post injury then once a week until the end of experiment (week 3). The BBB scaling score rates between 0 (paralysis) to 21 points (normal gait). Animals with scores more than four were excluded from the study. Natural recovery reflex is observed in rats within the hours to weeks post injury and they can take steps. In their hind limbs, the spinal circuits are able to develop a spinal reflex arc that lead to walking independently of the brain (Bazley et al. 2012; Tillakaratne et al. 2010). Based on this fact and also according to BBB rating scale (Basso et al. 1996), animals with scores more than four were excluded from the study. In this scale, score four represents slight movement of all three hind limb joints. In rats with scores more than four, extensive movement of the joints is observed, and final reason for animal exclusion is that in most clinical studies patients don't have any movement in their lower limbs and the design of animal studies should be close to the clinical trial studies.

Histological staining

SCI samples were embedded in paraffin (Merk, Germany) and serially sectioned (at the lesion epicenter (i.e. T10) and 0.5, 1, 1.5, and 2 mm rostral and caudal to the injury epicenter [24]) into 5 μm thick coronal slices with 50 μm interval. Specimens were then mounted and kept at 4 °C for further staining. A common hematoxylin and eosin (H&E) staining was carried out for histological confirmation of SCI model at day three post-injury. Nissl staining was performed for evaluation of neuronal cell death and density, Luxol Fast Blue (LFB) staining was carried out for analysis of white matter sparing at the injured area. Nissl and LFB staining were performed at 21 d post-SCI.

For Nissl staining, sections were deparaffinized in xylene, stained with cresyl violet, observed and photographed under an optical microscope (Labomed, USA). An imaging software (Soft imaging system, Berlin, Germany) was applied for further analysis of captured tissue samples. Neurons with obvious cytoplasm, clear nuclear borderline and visible nucleolus in the ventral horn of the spinal cord were counted for Nissl staining.

For LFB staining, sections were incubated with the LFB solution at 60 °C overnight. Then they were washed in dH_2O and further added to carbonate lithium for an additional 10 s. eventually, samples were transferred into crysol violet solution for 5 min and evaluated under a light microscope (Olympus, Tokyo, Japan). Quantification of the myelin diffusion outside the injury site was performed by ImageJ software (Soft Imaging System, Berlin, Germany).

Real-time quantitative PCR

Expression of NLRP1, NLRP3, ASC, active caspase-1, TNF-α, IL-1β and IL-18 genes were carried out. A Qiazol Lysis Reagent (Qiagen, USA) was used for extraction of total RNA from tissue specimens (10 mm long) containing injury epicenter according to manufacturer's protocols. The extracted RNA was then analyzed for purity by a NanoDrop 1000 instrument (PeqLap, Germany) analyzed by spectrophotometer (260/280 nm). One μg of total RNA from each sample was reverse-transcribed to cDNA using RevertAid First Strand cDNA Synthesis Kit (Thermo Scientific, USA). The reaction mixture for performing real-time analysis contained 2 μl cDNA, 1 μl primers (20 pmol/μL), 5 μl PCR Master Mix

(2X) (Korea, BioFact) and 2 μl RNAse-free water (Invitrogen, Germany). A ΔΔCt method was applied for estimation of relative quantification, and normalization of the real-time values was based on the expression for GAPDH as housekeeping. All primers were designed by Integrated DNA Technologies (Pishgam). List of primers and analyzed genes are presented in Table 1. Each experiment was performed in triplicate.

Western blotting

We used a SDS-PAGE for analysis of NLRP1, NLRP3, ASC and active caspase-1 using a western blot technique. First, total cellular proteins were lysed and extracted using lysis buffer (50 mM Tris–HCl, pH 8.0, 0.1% sodium dodecyl sulfate (SDS), 1% (*v*/v) Nonidet P-40 (Sigma, Igepal, CA), 0.5% sodium deoxycholate and protease inhibitor cocktail (Complete Mini, Roche, Mannheim, Germany)). The concentration of protein was obtained with a Total Protein Kit, Micro (sigma, USA), and about 20 μg/μL of these proteins were loaded and transferred onto PVDF membranes (Amersham, Cytomatin Gene, Iran). Incubation with a blocking buffer (1 ml glycerol +20 μL Tween 20 (T) + 40 mL Tris-buffered saline (TBS) 1X + 1 g skimmed milk) for 1 h was then exploited for blockade of unspecific proteins. Next, the membrane was overnight incubated with primary antibodies shown in Table 2, and then with a peroxidase-conjugated goat anti-rabbit (BioRad, USA) (Abcam, Germany) as secondary antibody for 90 min. Samples were visualized with an enhanced chemiluminescence method (ECL plus, Pierce Scientific, Waltham, MA, USA). GADPH was applied in the same blot technique for densitometeric measurements to normalize the intensities of specific bands using ImageJ software. The tissue specimens used for Western Blotting were same as RT-PCR.

Enzyme-linked immunosorbent assay (ELISA)

To determine serum levels of TNF-α, IL-1β and IL-18 cytokines, an ELISA technique was performed. Briefly, prior to

Table 1 List of primers used in this study

Primer	Sequence	Product size (bp)
Nlrp1a		131
F	ACCCCACCTTCCAAACAA	
R	CTGGCTAAGGGGCACATC	
Nlrp3		129
F	TCTTGAGGTCCACATCTTCC	
R	TTTTCATTCCTGCTCTGCC	
ASC		150
F	GGAGGGGTATGGCTTGGA	
R	TGTTCTGTTCTGGCTGTGC	
Casp-1		157
F	CGTCTTGCCCTCATTATC	
R	ATTCTTTTGTCATCTCCAG	
TNF-α		172
F	CACCACGCTCTTCTGTCT	
R	CGCTTGGTGGTTTGCTAC	
IL-1b		115
F	TCACTCATTGTGGCTGTGG	
R	GGACGGGCTCTTCTTCAA	
IL-18		129
F	ATGTCTACCCTCTCCTGT	
R	TTCCATTTTGTTGTGTCCTG	
GAPDH		121
F	AAGTTCAACGGCACAGTCAA GG	
R	CATACTCAGCACCAGCATCACC	

bp base pair length, *F* Forward, *R* Reverse, *Nlrp1a* NACHT, LRR and PYD domains-containing protein 1a, *Nlrp3* NACHT, LRR and PYD domains-containing protein 3, *ASC* apoptosis-associated speck-like protein containing a caspase activation, *Casp-1* Caspase-1, *TNF-α* tumor necrosis factor, *IL-1β* interleukin-1 beta, *IL-18* interleukin-18, *GAPDH* glyceraldehyde-3-phosphate dehydrogenase

Table 2 List of antibodies used in Western blot and ELISA

Antibody	Company	Cat. Number	Molecular Weight (kDA)
NLRP1	Novus, USA	NBP1–54899	170
NLRP3	Novus, USA	NBP1–12446	112
ASC	Proteintech Group, USA	10,500–1-AP	23
Active-caspase-1	Santa Cruz, USA	SC-56036	45
GAPDH	Sigma Aldrich	G8795	37
TNF-α	Proteintech Group, USA	17,590–1-AP	–
IL-1β	Proteintech Group, USA	16,806–1-AP	–
IL-18	R&D system, USA	AF521	–

scarification of animals, about 2 mL blood sample was collected. Samples were centrifuged (at 2000 rpm for 20 min at 4 °C), and serum was harvested for analysis of the cytokines using an ELISA kit (IL-1β, KE20005, proteintech, USA; TNF-α, KE20001, proteintech, USA; and IL-18, ABIN416245, antibodies-online.com). List of antibodies and molecular weight of used proteins in western blot is shown in Table 2.

Statistical analysis

All values are presented as mean ± SD. One-way analysis of variance (ANOVA) followed by Tukey's post-hoc was exploited for comparison of the differences between experimental groups using SPSS 24 software. $P < 0.05$ was considered statistically significant.

Results

Schwann cell morphology, identity and tracing

SCs investigated after three weeks of culture showed an elongated bipolar or tripolar shape with increased nuclear/cytoplasmic volume ratio. A lower number of more flattened fibroblast cells with polymorphic shape and larger nuclei

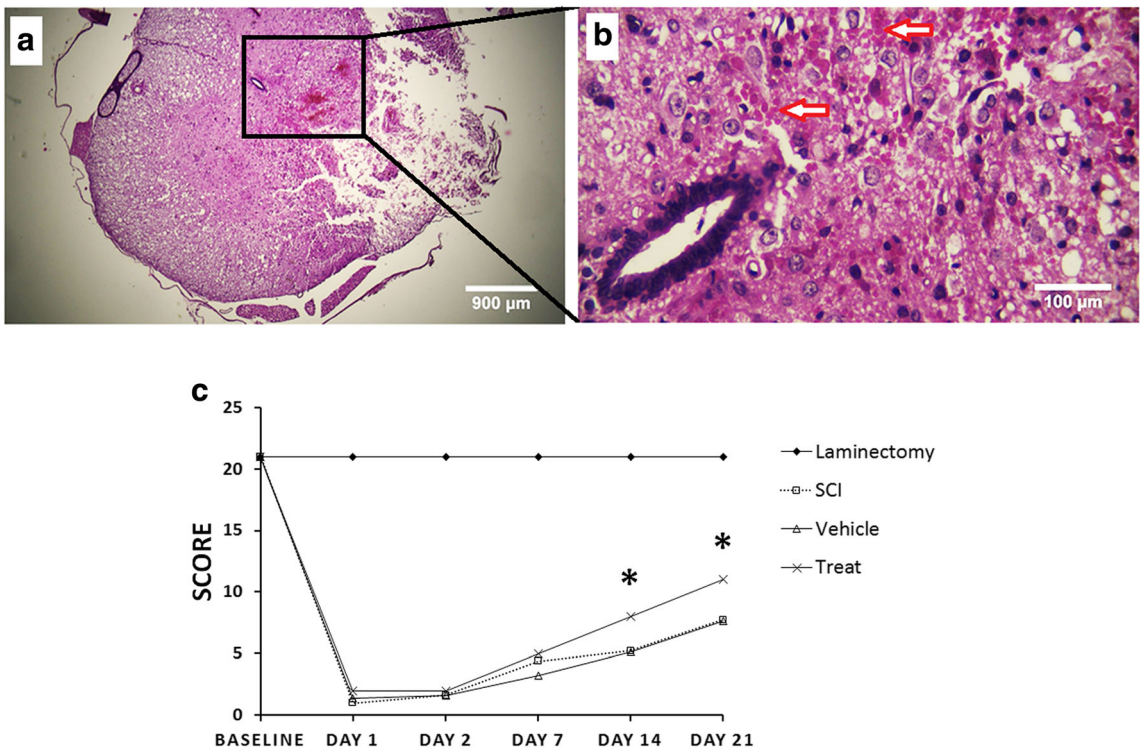

Fig. 2 Transverse section of the spinal cord at the level of T10 vertebral body and hind limb motor assessment (BBB open field score) in the study groups. a Showing cavity and b Arrows indicate bleeding, confirming the spinal cord injury (SCI) contusion model. Figure 2B was flipped and boxed area in picture A was enlarged. **a**, X40; and **b**, X400. **c** Effect of Schwann cell treatment on BBB scoring in the spinal cord injury (SCI) rats. Data are represented as mean ± SD ($n = 8$ per group). *$p < 0.05$ vs. SCI and vehicle

could also be seen between SCs (Fig. 1b). Identity of SCs was confirmed using ICC against S100, a cytoplasmic marker for the cells. The results revealed a purity of 98% ± 0.1 for the cells (Fig. 1c). Flow cytometry analysis was also checked for cell identity, and the results showed high expression for P75 NLGFr (96.68% ± 1.3) and S100 (97.77% ± 0.16), but low expression for CD45 (7.33% ± 3.21) and Thy-1 (7.21% ± 1.44) (Fig. 1d).

SCs injected to the injured area were traced fluorescently (CM-Dil). Homing assay showed labeled bright red SCs that migrated to the place of SCI via the spinal cord white matter parenchyma, confirming the presence and correct homing of the viable cells into injured areas (Fig. 1e).

SCI model induction

A common H&E staining was performed for histological confirmation of SCI model at day three post-injury. As it is observable from Fig. 2a and b, SCI caused cavity formation and bleeding in the injured site.

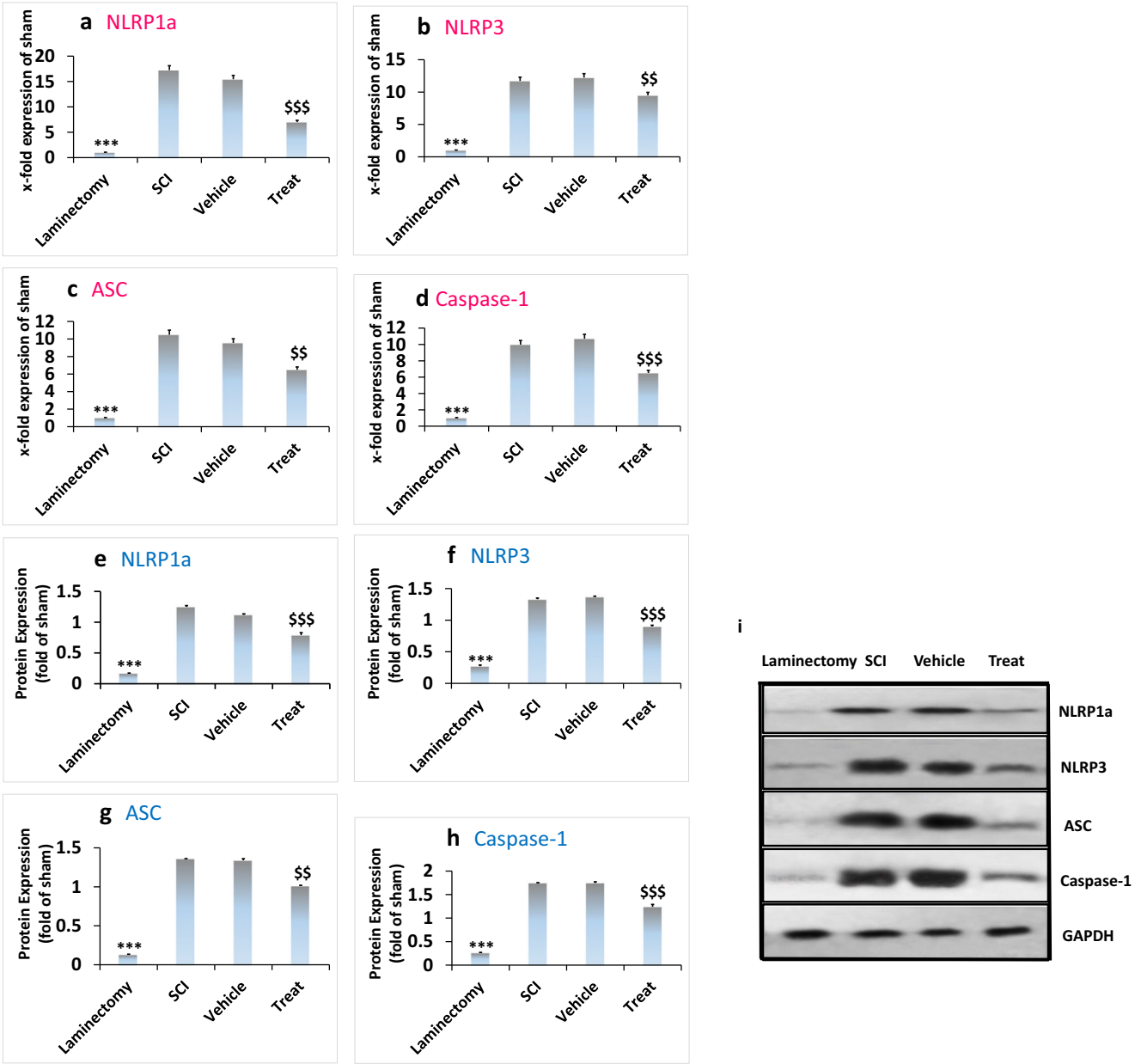

Fig. 3 Effect of Schwann cell treatment on NLRP1a, NLRP3, ASC and caspase-1 mRNAs and protein levels post spinal cord injury (SCI). Relative NLRP1a (**a**), NLRP3 (**b**), ASC (**c**) and caspase-1 (**d**) mRNA expressions were quantified with qRT-PCR, using GAPDH as an internal control for normalization. Western blot analysis shows quantitative assessment of NLRP1a (**e**), NLRP3 (**f**), ASC (**g**) and caspase-1 (**h**) proteins. **i** Representative western blots. Data represent mean ± SD. qRT-PCR, $n = 5$; and WB, $n = 4$. $^{\$\$}p < 0.01$, SCI and vehicle vs. treat; $^{\$\$\$}p < 0.001$, SCI and vehicle vs. treat; $^{**}p < 0.01$, SCI and vehicle vs. laminectomy; and $^{***}p < 0.001$ SCI and vehicle vs. laminectomy

Locomotor assessment

Locomotor activity and recovery were assessed using BBB locomotion rating scale. In the laminectomy group, the BBB score remained at the highest level (i.e. 21) throughout the study, while in the SCI group the score dropped to a level lower than 4, indicating a correct SCI procedure in animals. All animals exhibited a gradual improvement in the motor function especially after second week. The motor function was significantly improved after administration of Schwann cells, as compared to SCI and vehicle groups ($P < 0.05$) (Fig. 2c).

Roles for Schwann cell transplantation on inflammasome complexes in SCI model

The activation of inflammasome complexes by conversion of pro-caspase-1 to the active caspase-1 leads to release of inflammatory cytokines, and thereby initiating an inflammatory response (Petrilli et al. 2007), so the effects of SCs on the key inflammasome components (i.e. NLRP1a, NLRP3, ASC and caspase-1) were analyzed at both mRNA and protein levels at day 21 post-injury. SCI model considerably induced expressions for NLRP1a (Fig. 3a), NLRP3 (Fig. 3b), ASC (Fig. 3c) and caspase-1 (Fig. 3d) mRNAs, which were abrogated after transplantation of Schwann cells. The corresponding protein values were assessed by western blotting and showed a significant increase for NLRP1a (Fig. 3e), NLRP3 (Fig. 3f), ASC (Fig. 3g) and caspase-1 (Fig. 3h) proteins post-SCI, while the administration of SCs had a significant effect on reducing the levels for these proteins (Fig. 3e-h).

Effects of Schwann cell transplantation on inflammatory parameters in SCI model

Due to the fact that inflammasome activation is a trigger for caspase-1 cleavage that subsequently induces the activity for pro-inflammatory cytokines (i.e. TNF-α, IL-1β and IL-18) (Wen et al. 2012), our next trial was to assess the rates of expression for these cytokines at both mRNA and protein levels. SCI caused a significant increase in the mRNA expressions for the pro-inflammatory cytokines, which was counteracted after injection of SCs (Fig. 4a-c). This was also confirmed by ELISA. The only exception is for IL-18 protein, which was not significantly influenced by SCs in the injured area (Fig. 4d-f).

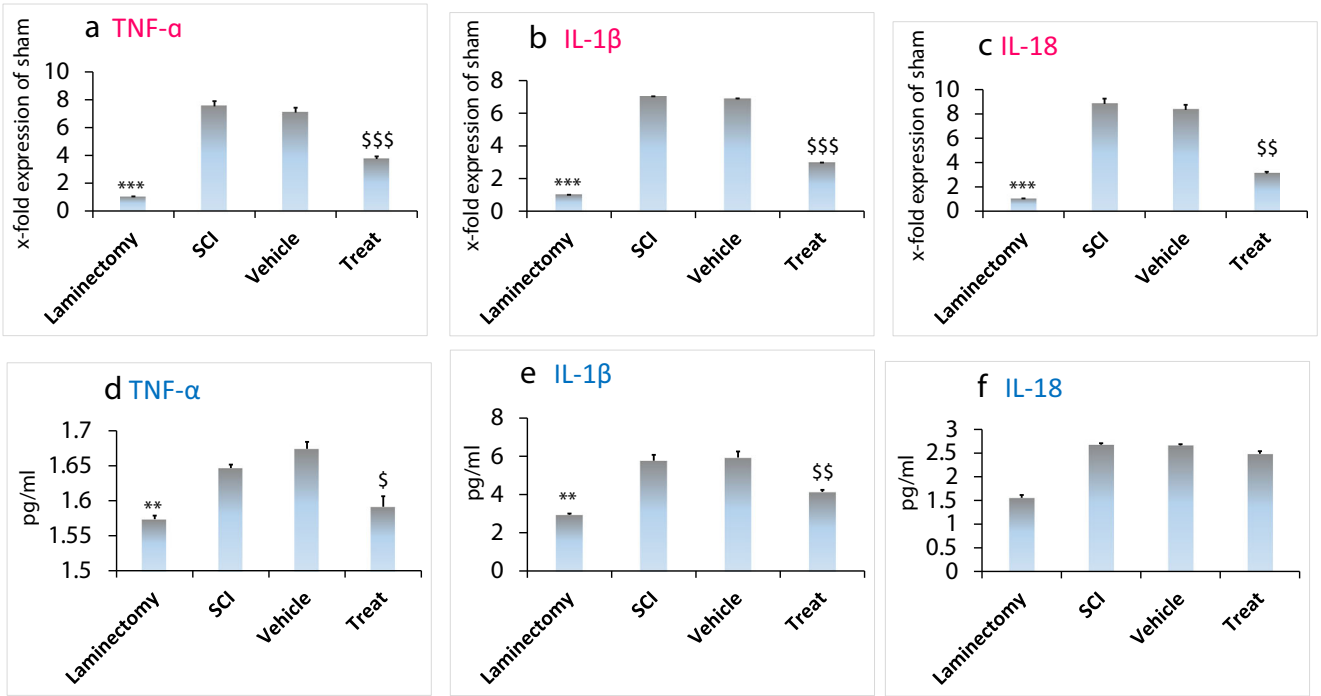

Fig. 4 Cytokine expression in the spinal cord after spinal cord injury (SCI) and Schwann cell transplantation. TNF-α (**a**), IL-1β (**b**) and IL-18 (**c**) mRNA expressions assessed by qRT-PCR, using GAPDH as the reference gene. TNF-α (**d**), IL-1β (**e**) and IL-18 (**f**) in the spinal cord were also evaluated for their protein expressions assessed by enzyme-linked immunosorbent assay (ELISA). Data are represented as mean ± SD. qRT-PCR, n = 5; and ELISA, n = 4. $^{\$}p < 0.05$, SCI and vehicle vs. treat; $^{\$\$}p < 0.01$, SCI and vehicle vs. treat; $^{\$\$\$}p < 0.001$, SCI and vehicle vs. treat; $^{**}p < 0.01$, SCI and vehicle vs. laminectomy; and $^{***}p < 0.001$, SCI and vehicle vs. laminectomy

Roles for Schwann cell transplantation on neuronal cell death in SCI model

Cell density of spinal ventral horn neurons was assessed by Nissl staining at third week post-SCI. As it is observable from the Fig. 5a, SCI caused a significant decrease in the number of surviving neurons, while this number was increased after treatment with Schwann cells. This was further confirmed by quantification of the Nissl staining. The number of cells stained positive for Nissl in the treatment group was 42.1 ± 4.21, which was considerable compared with the number for the SCI group with the number 11.9 ± 1.74 ($P < 0.001$) (Fig. 5b).

Myelination in the injured spinal cord after Schwann cell transplantation

LFB staining was performed in order to evaluate whether Schwann cell transplantation can preserve the existing myelin and/or promote myelination in the SCI rats at the end of week 3 of cell delivery. Severe damages to the myelin sheath along with decrease number of cells in the cystic areas formed in the gray matter were seen in the SCI group. The most affected sites for the SCI group were dorsal funiculus and dorsal horn. The number of cells within cystic areas in the grey matter was increased for the treatment group (Fig. 6a). LFB staining also showed that SCs induced axonal regeneration in the hollow region (Fig. 6a, last image). Quantification of LFB was carried out in order to determine whether the effects for Schwann cell transplantation on the mentioned changes were significant. As it could be seen the percentage of areas for LFB staining in the SCI group was 42.00 ± 2.89%, which was noticeable, as compared with the laminectomy group ($P < 0.001$). By contrast, the percentage for the treatment group was 66.85 ± 4.74%, which was significant ($P < 0.001$ vs. SCI group) (Fig. 6b).

Discussion

Inflammasome complexes including NLRP1 and NLRP3 have been reported for their delicate contribution to the pathogenesis of a variety of non- CNS diseases including renal fibrosis

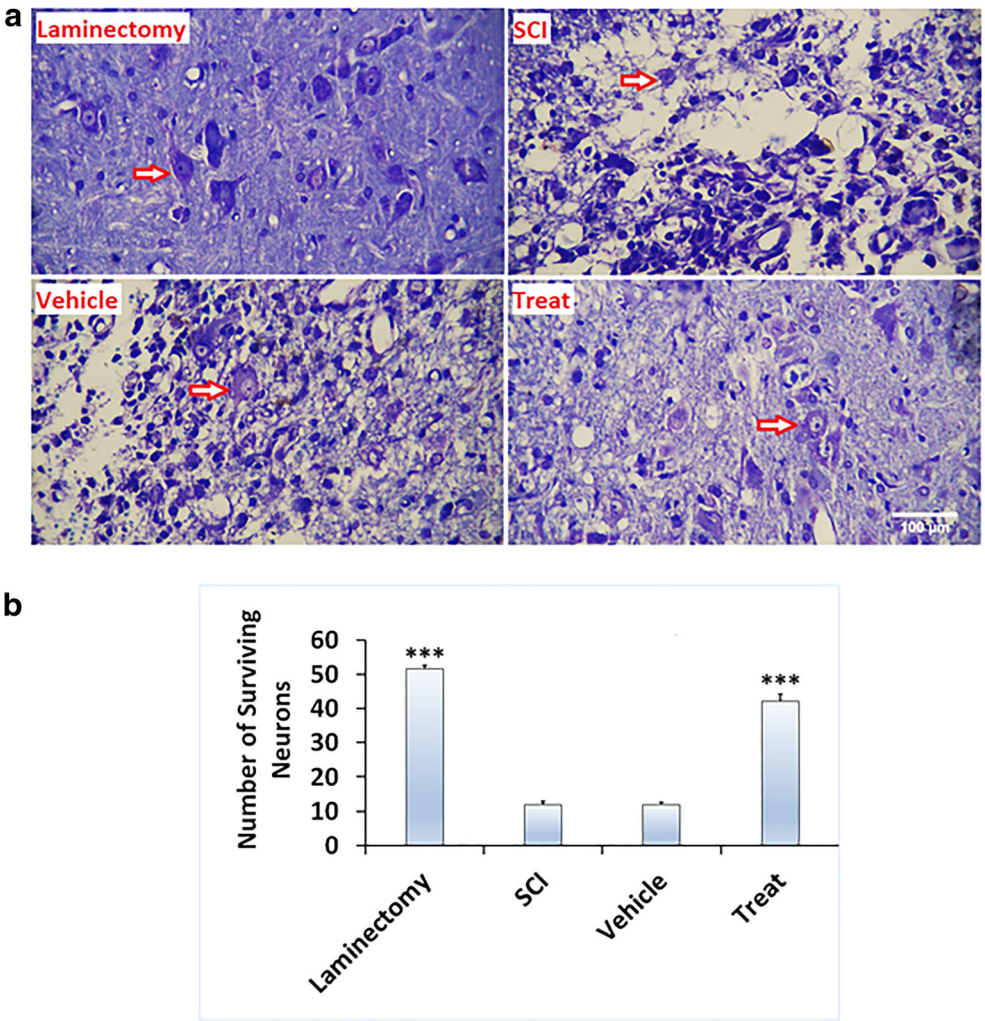

Fig. 5 Nissl staining for evaluation of neuronal cell density at the lesion site (spinal cord ventral horn) at 3 weeks post spinal cord injury (SCI) to survey the effects for Schwann cell administration on neuronal cell survival (**a**). Arrows indicate large healthy motor neurons. **b** Quantitative analysis of surviving motor neurons. $^{***}p < 0.001$ vs. SCI and vehicle. Data are represented as mean ± SD (n = 5 per animal)

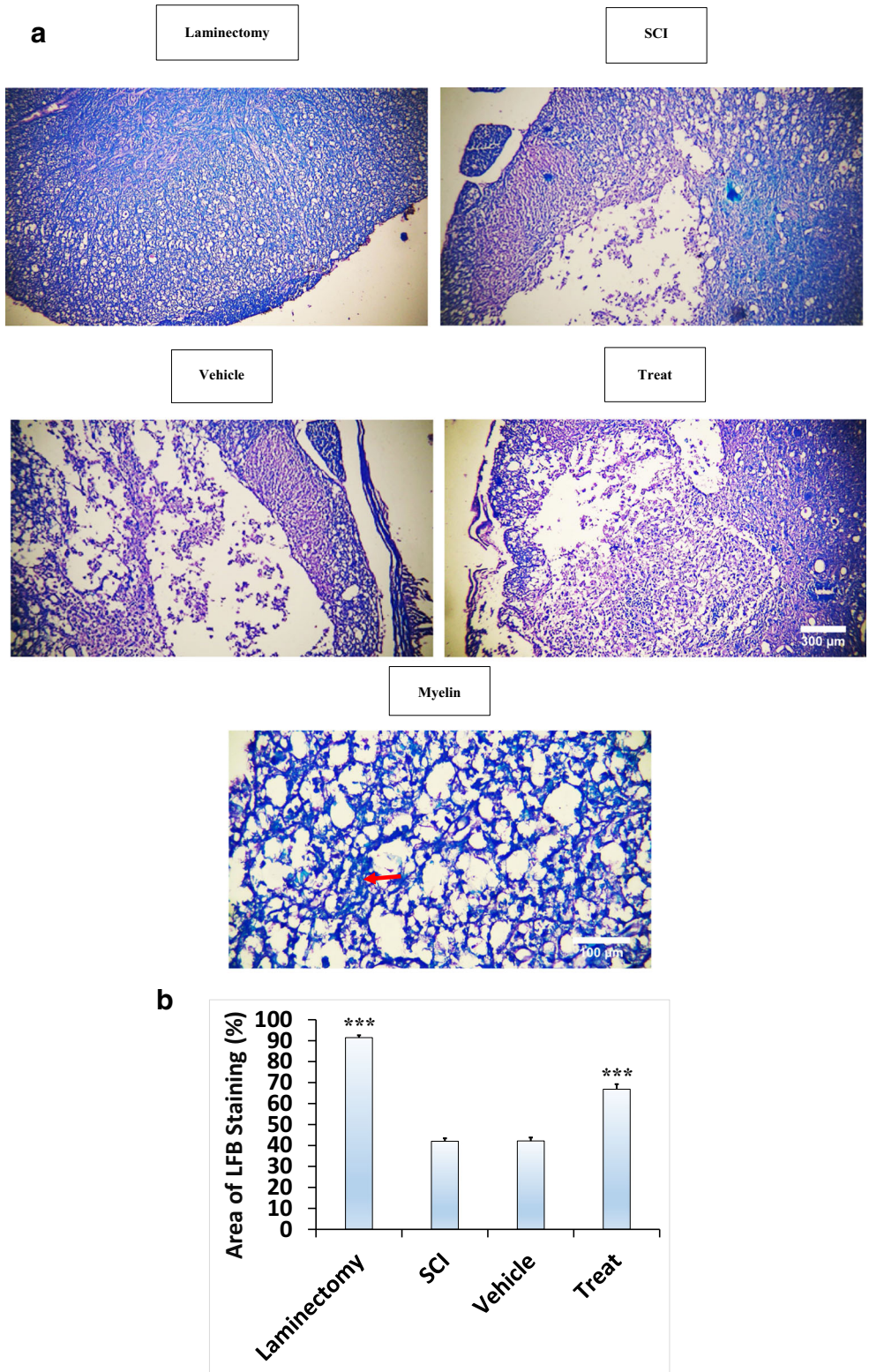

Fig. 6 Luxol fast blue (LFB) staining for analysis of white matter sparing at 3 weeks after Schwann cell delivery to the spinal cord injury (SCI) rats. LFB shows reduced white matter degeneration after cell therapy. **a** Representative images stained with LFB. Arrow indicate axon fibers that stained with LFB. **b** Quantitative analysis of myelinated areas. Data are represented as mean ± SD ($n = 7$ per group). $^{***}p < 0.001$ vs. SCI and vehicle

(Gong et al. 2016), pulmonary inflammation (Kang et al. 2017), bowel disease (Cocco et al. 2017), and also CNS diseases such as Alzheimer's disease (Lan et al. 2017), traumatic brain injury (TBI) (de Rivero Vaccari et al. 2009; Liu et al. 2013) and specially SCI (Bazrafkan et al. 2018; Jiang et al. 2017). Therefore, suppression of inflammasomes by different techniques such as hyperbaric oxygen therapy (Liang et al. 2015) or application of molecular/pharmacological products (de

Rivero Vaccari et al. 2008; Grace et al. 2016; Jiang et al. 2016b; Qian et al. 2017; Zendedel et al. 2016; Zhu et al. 2017) can be an optimistic approach for attenuating sensory/motor signs and symptoms.

In different studies, it has been proven that neuronal NLRP1 inflammasome is preassembled in the spinal cord under non-pathologic conditions or in non-stimulated neurons (Hsu et al. 2008), while NLRP3 inflammasome is activated following SCI (Ellis et al. 2016; Jiang et al. 2016a; Jiang et al. 2016b; Jiang et al. 2016c; Zendedel et al. 2016), and neurons and astrocytes begin to produce different chemokines and inflammatory cytokines (Pineau et al. 2010; Rice et al. 2007) causing localized progressive acute and chronic inflammation. This leads to disturbances in neuronal signaling and functional deficiency. As our research results showed, expressions for NLRP1, NLRP3 inflammasome components and pro-inflammatory cytokines were increased at both levels of mRNA and protein after SCI. Interestingly, we found more expression for NLRP1 mRNA than NLRP3 mRNA in SCI rats, while their protein expressions were almost the same. In our previous work, we found that NLRP3 was expressed in high amounts in the rat testis following SCI, but the expression of NLRP1 was not significant between the study groups. The difference between our two studies can be due to the different mechanisms of NLRP1 and NLRP3 inflammasomes in testicular and spinal cord tissues (Bazrafkan et al. 2018). Some studies also declared that NLRP3 is probably a dominant type of inflammsome activated in SCI, while the NLRP1 inflammasome is a dominant inflammasome for TBI (Mortezaee et al. 2018). There is no possible reason for similar expressions of NLRP1 and NLRP3 at protein levels following SCI. This may infer that the two type of inflammasomes are more active in gene levels. However, further investigations are required to shed more lights on the causative reasons for these outcomes.

We next examined whether Schwann cell transplantation could reduce tissue devastating effects (such as cell death and decreased myelination) and motor function impairment, all resulting from the activation of NLRP1, NLRP3 and further release of pro-inflammatory cytokines into extracellular space. In this study, we noticed attenuation for inflammasome components after administration of Schwann cells. The rate of decrease for NLRP1 and NLRP3 proteins after Schwann cell transplantation was almost the same, as it was for the SCI group, indicating equal contribution for the two inflammsomes in such therapeutic approach.

IL-18 and IL-1β are identified as key pro-inflammatory cytokines that are released after inflammasome activation in the SCI model (Mortezaee et al. 2018). Expression of IL-1β was effectively attenuated at both mRNA and protein levels after administration of Schwann cells. This was also happened for IL-18 mRNA. However, in this study, protein expression for this cytokine was not affected by cell transplantation, which may be due to the post translational modifications of proteins including folding, proteolytic cleavage, splicing and chemical (covalent) modification in the cell cytoplasm leading to differences found in the rate of expression between mRNA and protein for IL-18.

To further elucidate possible implication of Schwann cell transplantation for motor functional recovery, we tried to assay BBB and LFB testes. BBB is for evaluation of recovery in the hind limb locomotion that is regarded as a key measurement criterion for functional recovery in SCI model in rodents (Kachadroka et al. 2010). In the current study, SCI animals experienced impaired locomotion in hind limb joints, which was improved after application of Schwann cells. LFB staining carried out for white matter tissue sparing analysis also showed fewer numbers of cavities for treatment group. These cavities were occupied with neural aggregation along with regenerating myelinated axons. Relation between spared tissue and recovery in the hind limb locomotion is a complex phenomenon because of involvement of both upper and lower motor neuronal circuitry, such as intersegmental segmental and supraspinal elements (Kachadroka et al. 2010). Schwann cell transplantation has been reported to increase the number of myelinated axons in the lesion site, to decrease cystic cavities, and to increase white matter volume of the spinal cord (Myers et al. 2016). These cells are genetically engineered to produce high amounts of trophic factors or adhesion molecules implicated in improvement of motor function and spinal cord repair (Deng et al. 2013; Lavdas et al. 2010). Collectively, these data along with findings from Nissl staining that showed increased number of survival cells after cell administration indicate promising roles for Schwann cell transplantation for recovery of motor function by increasing neuronal survival and myelination in affected areas of SCI rats.

Our suggestion for future research in this area would be administration of SCs in a variety of numbers to get to know whether survival and viability of the transplanted cells in the injured area could influence outcomes. We also suggest to assay possible roles for Schwann cell transplantation on neural stem/progenitor cell proliferation and differentiation and its relation to inflammasome activation in the same model. Eventually, it would be impressive to investigate whether the use of exosomes instead of cell therapy could provide an appropriate alternative option for this context.

Conclusion

From these results we conclude that transplantation of Schwann cell to the contusive SCI model may provide promising results for attenuation of axonal demyelination and degeneration possibly through retarding the activity for inflammasome activation and related inflammatory circuit.

Acknowledgments This research was supported in part by a grant received from Tehran University of Medical Sciences and Health Services, Tehran, Iran (grant number: 95-01-30-31306).

Funding information Tehran University of Medical Sciences and Health Services, Tehran, Iran (grant number: 95–01–30-31,306).

Compliance with ethical standards

Conflict of interest The authors declare no potential conflicts of interest.

References

Anderson DK, Means ED, Waters TR, Green ES (1982) Microvascular perfusion and metabolism in injured spinal cord after methylprednisolone treatment. J Neurosurg 56:106–113

Arthur-Farraj PJ et al (2012) C-Jun reprograms Schwann cells of injured nerves to generate a repair cell essential for regeneration. Neuron 75: 633–647

Basso DM, Beattie MS, Bresnahan JC (1996) Graded histological and locomotor outcomes after spinal cord contusion using the NYU weight-drop device versus transection. Exp Neurol 139:244–256

Bazley FA et al (2012) Electrophysiological evaluation of sensory and motor pathways after incomplete unilateral spinal cord contusion. J Neurosurg Spine 16:414–423

Bazrafkan M et al (2018) Lipid peroxidation and its role in the expression of NLRP1a and NLRP3 genes in testicular tissue of male rats: a model of spinal cord injury. Iran Biomed J 22:151

Bergsbaken T, Fink SL, Cookson BT (2009) Pyroptosis: host cell death and inflammation. Nat Rev Microbiol 7:99

Campana WM (2007) Schwann cells: activated peripheral glia and their role in neuropathic pain. Brain Behav Immun 21:522–527

Chen L, Huang H, Xi H, Zhang F, Liu Y, Chen D, Xiao J (2014) A prospective randomized double-blind clinical trial using a combination of olfactory ensheathing cells and Schwann cells for the treatment of chronic complete spinal cord injuries. Cell Transplant 23: 35–44

Choobineh H, Gilani MAS, Pasalar P, Jahanzad I, Ghorbani R, Hassanzadeh G (2016) The effects of testosterone on oxidative stress markers in mice with spinal cord injuries. Int J Fertility Sterility 10:87

Choobineh H, Kazemi M, Gilani MAS, Heydari T, Shokri S, Bazrafkan M, Hassanzadeh G (2018) Testosterone reduces spinal cord injury-induced effects on male reproduction by preventing CADM1. Defect Cell J (Yakhteh) 20:138

Cocco M et al (2017) Development of an acrylate derivative targeting the NLRP3 Inflammasome for the treatment of. Inflammatory Bowel Disease J Medicinal Chemistry 60:3656–3671

De la Calle JL, Paíno CL (2002) A procedure for direct lumbar puncture in rats. Brain Res Bull 59:245–250

de Rivero Vaccari JP, Lotocki G, Marcillo AE, Dietrich WD, Keane RW (2008) A molecular platform in neurons regulates inflammation after spinal cord injury. J Neurosci 28:3404–3414

de Rivero Vaccari JP, Lotocki G, Alonso OF, Bramlett HM, Dietrich WD, Keane RW (2009) Therapeutic neutralization of the NLRP1 inflammasome reduces the innate immune response and improves histopathology after traumatic brain injury. J Cereb Blood Flow Metab 29:1251–1261

Deng L-X et al (2013) A novel growth-promoting pathway formed by GDNF-overexpressing Schwann cells promotes propriospinal axonal regeneration, synapse formation, and partial recovery of function after spinal cord injury. J Neurosci 33:5655–5667

Deng L-X, Walker C, Xu X-M (2015) Schwann cell transplantation and descending propriospinal regeneration after spinal cord injury. Brain Res 1619:104–114

Dubový P (2011) Wallerian degeneration and peripheral nerve conditions for both axonal regeneration and neuropathic pain induction. Annals of Anatomy-Anatomischer Anzeiger 193:267–275

Ellis A et al (2016) Morphine amplifies mechanical allodynia via TLR4 in a rat model of spinal cord injury. Brain Behav Immun 58:348–356

Fleshner M, Frank M, Maier SF (2017) Danger signals and inflammasomes: stress-evoked sterile inflammation in mood disorders. Neuropsychopharmacology 42:36

Gholaminejhad M, Arabzadeh S, Akbari M, Mohamadi Y, Hassanzadeh G (2017) Anti-oxidative and neuroprotective effects of flaxseed on experimental unilateral spinal cord injury in rat. J Contemporary Med Sci 3:213–217

Gong W, Mao S, Yu J, Song J, Jia Z, Huang S, Zhang A (2016) NLRP3 deletion protects against renal fibrosis and attenuates mitochondrial abnormality in mouse with 5/6 nephrectomy. American J Physiology-Renal Physiology 310:F1081–F1088

Grace PM et al (2016) Morphine paradoxically prolongs neuropathic pain in rats by amplifying spinal NLRP3 inflammasome activation. Proc Natl Acad Sci 113:E3441–E3450

Hassanzadeh G, Quchani SH, Sahraian MA, Abolhassani F, Gilani MAS, Tarzjani MD, Atoof F (2016) Leukocyte gene expression and plasma concentration in multiple sclerosis: alteration of transforming growth factor-βs, Claudin-11, and matrix Metalloproteinase-2. Cell Mol Neurobiol 36:865–872

Hsu L-C et al (2008) A NOD2–NALP1 complex mediates caspase-1-dependent IL-1β secretion in response to bacillus anthracis infection and muramyl dipeptide. Proc Natl Acad Sci 105:7803–7808

Jiang W et al (2016a) Quercetin suppresses NLRP3 inflammasome activation and attenuates histopathology in a rat model of spinal cord injury. Spinal Cord 54:592–596

Jiang W et al (2016b) Dopamine D1 receptor agonist A-68930 inhibits NLRP3 inflammasome activation, controls inflammation, and alleviates histopathology in a rat model of spinal cord injury. Spine 41: E330–E334

Jiang W et al (2016c) Neuroprotective effect of asiatic acid against spinal cord injury in rats. Life Sci 157:45–51

Jiang W, Li M, He F, Zhou S, Zhu L (2017) Targeting the NLRP3 inflammasome to attenuate spinal cord injury in mice. J Neuroinflammation 14:207

Kachadroka S, Hall AM, Niedzielko TL, Chongthammakun S, Floyd CL (2010) Effect of endogenous androgens on 17 β-estradiol-mediated protection after spinal cord injury in male rats. J Neurotrauma 27: 611–626

Kang MJ, Jo SG, Kim DJ, Park JH (2017) NLRP3 inflammasome mediates interleukin-1β production in immune cells in response to Acinetobacter baumannii and contributes to pulmonary inflammation in mice. Immunology 150:495–505

Kreider B, Messing A, Doan H, Kim S, Lisak R, Pleasure D (1981) Enrichment of Schwann cell cultures from neonatal rat sciatic nerve by differential adhesion. Brain Res 207:433–444

Kuo H-S et al (2011) Acid fibroblast growth factor and peripheral nerve grafts regulate Th2 cytokine expression, macrophage activation, polyamine synthesis, and neurotrophin expression in transected rat spinal cords. J Neurosci 31:4137–4147

Lan Z, Xie G, Wei M, Wang P, Chen L (2017) The protective effect of Epimedii folium and Curculiginis Rhizoma on Alzheimer's disease by the inhibitions of NF-κB/MAPK pathway and NLRP3 inflammasome. Oncotarget 8:43709

Lavdas AA, Chen J, Papastefanaki F, Chen S, Schachner M, Matsas R, Thomaidou D (2010) Schwann cells engineered to express the cell adhesion molecule L1 accelerate myelination and motor recovery after spinal cord injury. Exp Neurol 221:206–216

Liang F, Li C, Gao C, Li Z, Yang J, Liu X, Wang Y (2015) Effects of hyperbaric oxygen therapy on NACHT domain-leucine-rich-repeat- and pyrin domain-containing protein 3 inflammasome expression in rats following spinal cord injury. Mol Med Rep 11:4650–4656

Liu H-D et al (2013) Expression of the NLRP3 inflammasome in cerebral cortex after traumatic brain injury in a rat model. Neurochem Res 38:2072–2083

Martinon F, Burns K, Tschopp J (2002) The inflammasome: a molecular platform triggering activation of inflammatory caspases and processing of proIL-β. Mol Cell 10:417–426

Mirsky R et al (2002) Schwann cells as regulators of nerve development. J Physiology-Paris 96:17–24

Mortazavi MM, Harmon OA, Adeeb N, Deep A, Tubbs RS (2015) Treatment of spinal cord injury: a review of engineering using neural and mesenchymal stem cells. Clin Anat 28:37–44

Mortezaee K, Khanlarkhani N, Beyer C, Zendedel A (2018) Inflammasome: its role in traumatic brain and spinal cord injury. J Cell Physiol 233:5160–5169

Myers SA, Bankston AN, Burke DA, Ohri SS, Whittemore SR (2016) Does the preclinical evidence for functional remyelination following myelinating cell engraftment into the injured spinal cord support progression to clinical trials? Exp Neurol 283:560–572

Nikmehr B et al (2017) The correlation of gene expression of inflammasome indicators and impaired fertility in rat model of spinal cord injury: a time course study. Urol J 14:5057–5063

Norenberg MD, Smith J, Marcillo A (2004) The pathology of human spinal cord injury: defining the problems. Mary Ann Liebert, Inc

Oraee-Yazdani S et al (2016) Co-transplantation of autologous bone marrow mesenchymal stem cells and Schwann cells through cerebral spinal fluid for the treatment of patients with chronic spinal cord injury: safety and possible outcome. Spinal Cord 54:102–109

Petrilli V, Papin S, Dostert C, Mayor A, Martinon F, Tschopp J (2007) Activation of the NALP3 inflammasome is triggered by low intracellular potassium concentration. Cell Death Differ 14:1583

Pineau I, Sun L, Bastien D, Lacroix S (2010) Astrocytes initiate inflammation in the injured mouse spinal cord by promoting the entry of neutrophils and inflammatory monocytes in an IL-1 receptor/MyD88-dependent fashion. Brain Behav Immun 24:540–553

Pishva AA et al (2016) Effect of estrogen therapy on TNF-α and iNOS gene expression in spinal cord injury model. Acta medica Iranica 54: 296–301

Profyris C, Cheema SS, Zang D, Azari MF, Boyle K, Petratos S (2004) Degenerative and regenerative mechanisms governing spinal cord injury. Neurobiol Dis 15:415–436

Qian J, Zhu W, Lu M, Ni B, Yang J (2017) D-β-hydroxybutyrate promotes functional recovery and relieves pain hypersensitivity in mice with spinal cord injury. Br J Pharmacol 174:1961–1971

Rice T, Larsen J, Rivest S, Yong VW (2007) Characterization of the early neuroinflammation after spinal cord injury in mice. J Neuropathol Exp Neurol 66:184–195

Saberi H et al (2011) Safety of intramedullary Schwann cell transplantation for postrehabilitation spinal cord injuries: 2-year follow-up of 33 cases. J Neurosurg Spine 15:515–525

Sekhon LH, Fehlings MG (2001) Epidemiology, demographics, and pathophysiology of acute spinal cord injury. Spine 26:S2–S12

Shamash S, Reichert F, Rotshenker S (2002) The cytokine network of Wallerian degeneration: tumor necrosis factor-α, interleukin-1α, and interleukin-1β. J Neurosci 22:3052–3060

Shen A et al (2008) Lipopolysaccharide-evoked activation of p38 and JNK leads to an increase in ICAM-1 expression in Schwann cells of sciatic nerves. FEBS J 275:4343–4353

Taskinen H, Olsson T, Bucht A, Khademi M, Svelander L, Röyttä M (2000) Peripheral nerve injury induces endoneurial expression of IFN-γ, IL-10 and TNF-α mRNA. J Neuroimmunol 102:17–25

Tillakaratne NJ et al (2010) Functional recovery of stepping in rats after a complete neonatal spinal cord transection is not due to regrowth across the lesion site. Neuroscience 166:23–33

Tofaris GK, Patterson PH, Jessen KR, Mirsky R (2002) Denervated Schwann cells attract macrophages by secretion of leukemia inhibitory factor (LIF) and monocyte chemoattractant protein-1 in a process regulated by interleukin-6 and LIF. J Neurosci 22:6696–6703

Tschopp J, Schroder K (2010) NLRP3 inflammasome activation: the convergence of multiple signalling pathways on ROS production? Nat Rev Immunol 10:210

Wen H, Ting JP, O'neill LA (2012) A role for the NLRP3 inflammasome in metabolic diseases—did Warburg miss inflammation? Nat Immunol 13:352

Zendedel A, Johann S, Mehrabi S, M-t J, Hassanzadeh G, Kipp M, Beyer C (2016) Activation and regulation of NLRP3 inflammasome by intrathecal application of SDF-1a in a spinal cord injury model. Mol Neurobiol 53:3063–3075

Zhang K-J, Zhang H-L, Zhang X-M, Zheng X-Y, Quezada HC, Zhang D, Zhu J (2011) Apolipoprotein E isoform-specific effects on cytokine and nitric oxide production from mouse Schwann cells after inflammatory stimulation. Neurosci Lett 499:175–180

Zhang H-Y et al (2013) Regulation of autophagy and ubiquitinated protein accumulation by bFGF promotes functional recovery and neural protection in a rat model of spinal cord injury. Mol Neurobiol 48: 452–464

Zhou X-H et al (2012) Transplantation of autologous activated Schwann cells in the treatment of spinal cord injury: six cases, more than five years of follow-up. Cell Transplant 21:S39–S47

Zhu Y, Zhu H, Wang Z, Gao F, Wang J, Zhang W (2017) Wogonoside alleviates inflammation induced by traumatic spinal cord injury by suppressing NF-κB and NLRP3 inflammasome activation. Experimental and Therapeutic Medicine 14:3304–3308